

Neural network forecast of the sunspot diagram

Eurico Covas^a, Nuno Peixinho^{a,b}, João Fernandes^{a,c}

^a*Centro de Investigação da Terra e do Espaço da University of Coimbra (CITEUC), Geophysical and Astronomical Observatory, University of Coimbra, 3040-004, Coimbra, Portugal*

^b*Unidad de Astronomía, Facultad de Ciencias Básicas, Universidad de Antofagasta, Chile*

^c*Department of Mathematics, University of Coimbra, 3001-454, Coimbra, Portugal*

Abstract

We attempt to forecast the Sun's sunspot butterfly diagram using neural networks as a prediction method. We use this approach to forecast in both latitude (space) and time, using a full spatial-temporal series of the sunspot diagram from 1874 to 2015 that trains the neural network. The analysis of the results show that it is indeed possible to reconstruct the overall shape and amplitude of the spatial-temporal pattern of sunspots using these feed-forward neural networks. However, we conclude that more data and/or improved neural network techniques are probably necessary for this approach to have real predictive power.

Keywords: magnetic fields, (Sun:) sunspots, Sun: magnetic fields, Neural networks

Email addresses: eurico.covas@mail.com (Eurico Covas),
nuno.peixinho@gmail.com (Nuno Peixinho), jmfernan@mat.uc.pt (João Fernandes)
URL: www.euricocovas.com (Eurico Covas)

1. Introduction

The sunspots are mostly a visible phenomenon in the solar photosphere and a manifestation of solar activity. One can find extensive bibliography about the solar cycle, its causes and consequences. Here we emphasise just a few number of previous results and further detail can be obtained in the recent reviews Hathaway (2015a,b) and references therein. Since the seminal work of George Ellery Hale in 1908 named “On the Probable Existence of a Magnetic Field in Sun-Spots” (Hale, 1908) it is known that sunspots contains strong magnetic fields, ascending from the interior to the surface. These intense magnetic fields will decrease the energy flux considerably and so the sunspots appear darker than the surroundings.

Other than the physical nature, we know, since Schwabe (1844), that the rise of the sunspots in the solar surface is cyclic but not periodic, with erratic time laps between maxima and/or minima that can span between 9 to 13 years. However, one can establish an average period time of about 11 years. Moreover, thanks to the analysis of the cosmogenic isotopes, e.g. ^{14}C and ^{10}Be (Beer et al., 1998) it is possible to reconstruct the solar cycle back to more than 10,000 years which is particularly interesting for paleoclimatology (Solanki et al., 2004), where other long period cycles emerge like Gleisseberg (around 88 years), Suess (around 208) or Hallstatt (around 2200 years) among others. Recently, Luthardt and Rößler (2017) has shown some evidence that there is a cycle around 11 years on 300-million-year fossilised tree rings. This could mean that the sunspot cycle (which affects cosmic radiation input to the Earth’s atmosphere, possibly causing an impact on cloud formation and therefore on annual rates of precipitation) has been around for a much longer

time scale than our current direct observation record.

On the other hand, the sunspot cycle is one of the cornerstone results in natural sciences where implications are far beyond to only the interest of astronomers and physicists. Zhou et al. (1998) studied the relationship between the solar cycle length and tree-ring concluding that wider tree-rings are associated with shorter sunspot cycles; it is known the work of Alexander Leonidovich Tchijevsky who support the idea of a connection between the solar cycle and mass activity of peoples (Kornbluh, 1965); in economics one can find the concept “sunspot equilibrium” introduced by Cass and Shell (1983), where the market outcome varies in a way unrelated to economic fundamentals parameters or variables; the sunspot time series is often used to test forecast techniques such as the autoregressive integrated moving average (Box and Jenkins, 1976; Zhang, 2003) and other techniques, since it is the longest continuously recorded daily measurement made in science (Owens, 2013); it is clearly established that the solar activity can have a direct impact on social and economic activities through space weather phenomena, with particular relevance in electric grids, electronic devices and Global Navigation Satellite System (GNSS) navigation (Schrijver, 2015).

The impact of the sunspot cycle in fundamental science and its applications make the forecasting of the solar activity of major importance. However, the causes of the solar cycle are still an open question and widely studied. We can find in literature what we can name as the endogenous causes, where solar dynamo takes the main role - see e.g. Parker (1979) and for reviews see Ossendrijver (2003b,a) - and the exogeneous ones, as the controversial theory about the effect of the planetary dynamics in the internal

structure of Sun - see e.g. Abreu et al. (2012), Poluianov and Usoskin (2014) and for reviews see Charbonneau (2013).

The predictions or forecasting methods can be divided between pure mathematical methods - see e.g. Kane (1999); Ogurtsov (2005a,b), and methods based on some physical mechanism descriptions (see e.g. Schatten, 2005; Svalgaard et al., 2005; Dikpati et al., 2006, and references therein), particularly the dynamo theory - see e.g. Parker (1979) and for reviews see Ossendrijver (2003b,a). For procedures based on a combination of mathematical and physical approaches see e.g. Hathaway and Wilson (2006) and Duhau (2003).

There is quite a large body of research on forecasting the sunspot time series, in particular the strength, the length and the maximum of the next cycle. However, one can see from the results of the American Geophysical Union (AGU) meeting in December 2008 that there seems to be almost more forecasts than possible future data scenarios, as shown in the “piano plot” presented by W. D. Pesnell who has summarized the literature for predictions of the cycle 24’s maximum sunspot number (see Pesnell, 2008, 2012). Depending on the most realistic maximum number of sunspots (Acero et al., 2017), one would think that there are more articles predicting the next cycle sunspot number maximum than attainable physical possibilities. Pesnell’s plot emphasises that metrics such as the sunspot number (or others related ones such as the average sunspot number or total sunspot area coverage) may not contain enough information to decided among distinct forecasting methods.

It was under these motivations that one of us (Covas, 2017) attempted to use a model based on spatial-temporal embeddings to forecast the so called

sunspot butterfly diagram, and demonstrated a pure mathematical model to predict the butterfly diagram doing a two-dimensional forecast (time versus latitude), based on the full data set for the sunspot areas and its latitudinal position, from 1874 to 2015. That work, however, was not the first one to attempt to predict or reconstruct the entire sunspot butterfly diagram (space and time, not just time). Jiang et al. (2011) analysed the butterfly diagram in its entirety to calculate correlations between the latitude, longitude, area, and tilt angle of sunspot groups against the cycle strength and phase. With those correlations they were then able to reconstruct the sunspot butterfly diagram. This reconstruction was successful for both weak and strong cycles and this ability to reconstruct (or predict) both weak, medium, and strong cycles is very important and we shall come back to this point later in this article.

In this article, we propose an approach by forecasting the full sunspot butterfly diagram, using the same data as in Covas (2017) by means of neural networks techniques. Several authors have already attempted to use neural networks to forecast aspects of the sunspot cycle, although none in both space and time, having restricted themselves to mostly sunspot number or areas, i.e., forecasts in time only. Villarreal and Baffes (1990) describes earlier attempts to predict sunspot activity using neural networks at NASA. Koons and Gorney (1990) used a neural network simulation to predict the maximum 13-month smoothed sunspot number for cycle 22. Weigend (1991) (see also Weigend et al., 1992) showed one of the first attempts to forecast sunspot series and how to reduce complexity by pruning the number of weights or neuron connections. MacPherson (1993) (see also Li et al., 1990; Macpherson

et al., 1995) presented also one of the first attempts to use neural networks to model the pattern of the sunspot series. Conway (1994) demonstrated a possible problem with neural network forecasting applied to sunspot time series whereby the network basically produces trivial forecasts. Navone and Ceccatto (1995) and Calvo et al. (1995) attempted to forecast the solar cycle 22 and 23 sunspot number using neural networks while using the embedding dimension of the sunspot time series as way to define the architecture of the input layer. Koskela et al. (1996) used different types of neural networks, including feed-forward neural networks; finite impulse response (FIR) network, where the neuron synapse weights are replaced by finite impulse response filters; and an Elman network, one that has connections between units that form a directed cycle, to forecast the sunspot numbers among other non-linear time series. Fessant et al. (1996b) (see also Fessant et al., 1996a) used a neural network to predict aspects of the ascending phase of cycle 22 and compared its performance with other methods. Park et al. (1996) examined the relationship between the number of hidden neurons and the forecast, using sunspot number data. Kulkarni et al. (1998) predicted weaker solar cycle 23 activity using a feed-forward neural network calibrated with a state space non-linear reconstruction. Conway et al. (1998) (see also review in Conway, 1998) used a feed-forward neural network to predict the sunspot number 1 to 6 years ahead for solar cycle 23. Verdes et al. (2000) (see also Verdes et al., 2004) attempted to predict the near-maximum and declining activity of solar cycle 23 by means of a neural network. Lundstedt (2001) presented an interesting neural networks approach to predict the solar activity using SOHO/MDI high resolution solar magnetic field data. Small and Tse (2002)

showed a technique to calculate the minimum number of neurons to model the sunspot number time series and therefore avoid overfitting. Mordvinov et al. (2004) used neural networks to reconstruct sunspot indices as well the total solar irradiance. Gholipour et al. (2005) (see also Attia et al., 2004; Quassim and Attia, 2005; Attia et al., 2005; Mirmomeni et al., 2006; Quassim et al., 2007; Attia et al., 2013) used a neural network with multisteps to predict long-term sunspot number time series. Xie et al. (2006) used a adaptive time-delay neural network model for the prediction of sunspot series. Maris and Oncica (2006) presented a forecast of both sunspot numbers and several geomagnetic indices for solar cycle 24. Emmert-Streib and Dehmer (2007) (see also Pandya et al., 1997) presented a forecast analysis of sunspot numbers and the implications of having noise on the inputs to the neural network. Lundstedt et al. (2006) and Wik (2008) showed an application of neural networks for prediction of the solar magnetic flux, a physical variable which is correlated with sunspots. Gang and Shi-Sheng (2007) applied neural networks for forecasting the solar cycle 23. Uwamahoro et al. (2009) attempted to predict the solar cycle 24 using the neural networks and also used it to establish a relationship between a geomagnetic index and the sunspot number. Francile and Luoni (2010) (see also Parodi et al., 1999) examined in detail the sensitivity of the neural network to the topology used and other architectural parameters when predicting the sunspot number time series. Ajabshirizadeh et al. (2011) (see also Ajabshirizadeh and Juzdani Nafiseh, 2010) used a feed-forward network to predict the solar sunspot number and in particular the maximum occurrence and its value for solar cycle 24. Both Chattopadhyay et al. (2011) and Jiang and Song (2011) used the yearly mean

sunspot numbers and applied a neural network to forecast, comparing the results to other numerical methods. Maslennikova and Bochkarev (2012) and Maslennikova and Bochkarev (2014) presented long-term predictions of sunspot number time series based on singular spectral analysis and neural networks. Chandra and Zhang (2012) (see also Park and Woo, 2009; Kim et al., 2010; Moghaddam et al., 2013) used a different type of network, a recurrent neural network, to forecast the sunspot numbers and demonstrate the performance of this method. Chattopadhyay and Chattopadhyay (2012) used statistical analysis of monthly sunspot number time series with neural networks and compared its performance against autoregressive models while Ding et al. (2012) used neural networks to forecast the smoothed monthly mean sunspot area instead of the sunspot numbers. Liu and Du (2012) used quantum particle swarm and neural networks to forecast the sunspot number time series. Gkana and Zachilas (2015) and Zachilas and Gkana (2015) used the average mutual information and the false nearest neighbours' methods to estimate the suitable embedding parameters and then apply a neural network to forecast the peak of the present cycle 24. Finally (Parsapoor et al., 2015a,b) attempted to predict the cycle 24 time series using a connectionist model of the emotional system while (Li and Wang, 2017) used ensemble mode decomposition and wavelet neural network to forecast sunspot numbers. All of articles in the extensive list above, however, limited themselves to forecasts in time only, not space and time. So, as said in this article we attempt to forecast the full sunspot butterfly diagram, by means of neural networks. We believe that by including one further dimension to the usual one-dimensional forecasts prevalent in the literature, one should, in the fu-

ture, be able to decide better between the multitude of forecasting methods.

In Section 2 we describe the general method of forecasting using neural networks and in particular the application to a two-dimensional data set (one spatial, one temporal dimension). In Section 3 we apply the method to the sunspot area coverage latitude-time data set and in Subsection 3.2 we describe how the method’s parameters can be auto-calibrated using two statistical measures. Finally, in Section 4 we conclude and proposed possible future research avenues.

2. The method: feed-forward neural networks

Here we propose an approach which is based on artificial neural networks - Lecun et al. (1998); Krizhevsky et al. (2012) (for a review see Reed and Marks II, 1999). We use a subset of neural networks called feed-forward artificial neural networks. These are basic networks that have a input layer, one or more hidden layers and an output layer, fully connected but where no connection occurs backwards or on a loop (see Fig. 1 for a simplified example). Information flows from input to hidden and from hidden to output layers. The input layer takes input data, patterns of data that have a target output, i.e., a known result. The input layer nodes are connected to one (or more) hidden layer nodes, via weights and a nonlinear activation or “squash” function. Then the hidden layer nodes are connected via another set of weights and another nonlinear activation function to an output layer. For each neuron, the sum of the products of the weights by the preceding neurons is calculated, and then the value is passed via the activation function, typically a logistic or tanh function. Functions with simple known analytical

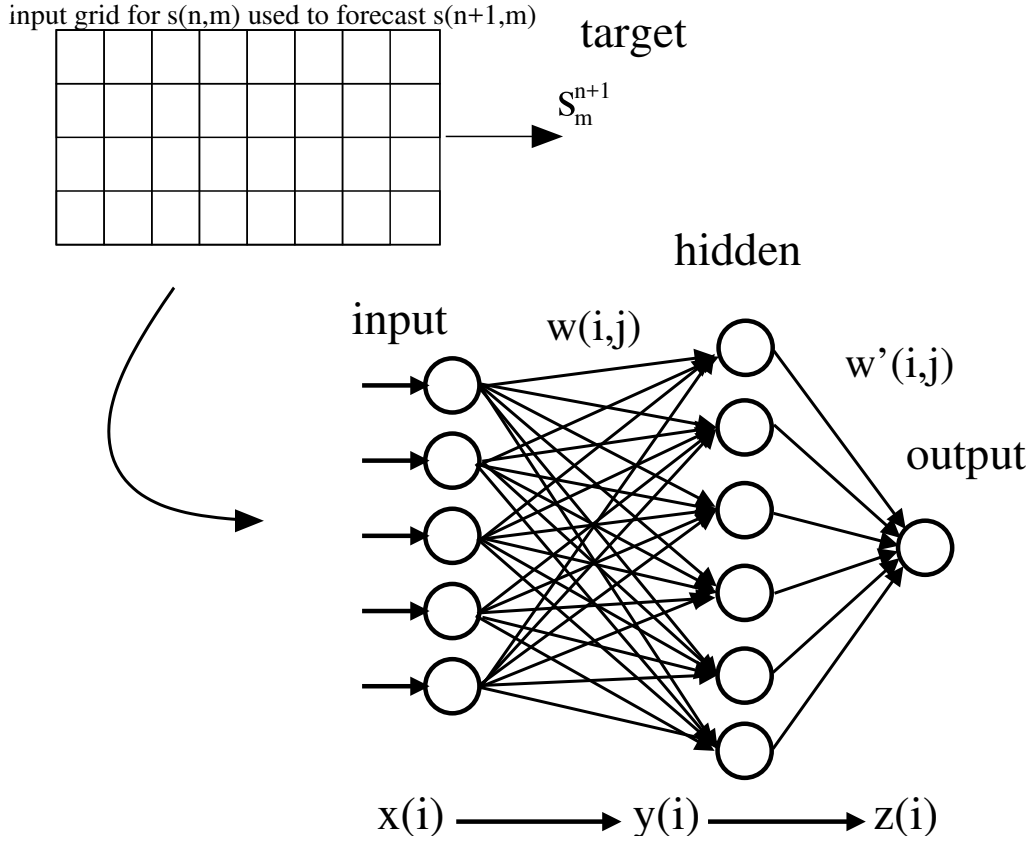


Figure 1: Forecasting method illustration. The neural network is made of an input layer, one or more hidden layer(s) and one output layer. In this article, we use only one hidden layer and the output layer is made of a single neuron. Each input pattern $x(i)$ is sent to the input layer, then each of the hidden neurons values is calculated from the sum of the product of the weights by the inputs $\sum w(i,j)x(i)$ and passed via the activation function. Then the output is made by the product of the second set of weights times the hidden node values $\sum w'(i,j)y(i)$ again passed to another (or the same) activation function. Each input pattern $x(i)$ is actually a matrix constructed using an embedding space of spatial and temporal delays, calculated from the actual physical spatial-temporal data values $s(n,m)$. After many randomly chosen input patterns are passed via the neural network, the weights hopefully converge to an optimal training value.

derivatives are preferred (Nielsen, 1987). There are several methods to train a network, the most commonly used being the back-propagation algorithm (Rumelhart et al., 1986; Rumelhart et al., 1986). In this method, the output values from the output layer are compared with the target via some predefined error function. The weights are then adjusted via a gradient descent method (see Reed and Marks II, 1999, and references therein). In order to use this method, the derivatives of the error function with respect to the network weights are calculated, and the weights are changed such that the error decreases. Therefore, error functions which are smooth and differentiable are preferred. Furthermore, there are several different free parameters, e.g. the rate of learning (the scaling of the derivative of the error with respect to weights) - the so called η parameter, the rate of momentum or inertia α - a kind of stubbornness in the human analogy, and the rate of forgetfulness ρ on the network (see Reed and Marks II, 1999, and references therein for details).

So that the network converges to a good solution, one needs to pass as much patterns (input/target pairs) as possible. There are two main types of training, batch and on-line training (see Reed and Marks II, 1999, and references therein). In the former we pass all patterns in one go and the change of weights is calculated based on the sum of errors, while for the latter, the weights are updated for each pattern. The on-line training is now the recommended approach in the literature (Wilson and Martinez, 2003) and it corresponds to some kind of random gradient descent method allowing for the possibility to jump out of local minima by having a kind of stochastic bump. In on-line training, patterns should be presented to the neural network

in random sequence and can be repeated. Training a neural network is still more of an art than a science, given the possible problems such as lack of convergence, local minima, no agreed theoretical approach/formula for the number of input/hidden/output neurons, the number of hidden layers and in general the architecture of the network. There are also problems with underfitting, overfitting, when to stop the training, which activation and error functions to use and how to specify the rate of learning, momentum and forgetfulness, among others. Also, the problem could have a sensitivity to the initial values of the weights and the order of the training patterns. Overall, in this article, we try to keep the approach as simple as possible, to avoid conditioning the solution.

Most of the neural network literature on forecasting focus on temporal forecasts, i.e., the data is a pure time series with no spatial components (Kaastra and Boyd, 1996). Most of the attempts to forecast in time are divided into two groups, one using time delays (Kim et al., 1999) to construct the vector input patterns for the feed-forward neural network, and another using what is called a recurrent network (Elman, 1990), where the information is allowed to cycle in a loop (Koskela et al., 1996; Petrosian et al., 2000; Zhang and Xiao, 2000; Han et al., 2004; Zhang, 2009; Chandra and Zhang, 2012). Here we shall use only the former, mainly for simplicity and easiness of implementation. The time delay approach in the literature uses the embedding dimension and sometimes the derived time lags to create an appropriate set of input patterns (Lin et al., 1992; Leung and Lo, 1993; Kulkarni et al., 1997; Saad et al., 1998; Wintoft and Cander, 1999; Annunziato et al., 2000; Sitte and Sitte, 2000; Frank et al., 2001; Elshorbagy et al., 2002; Shi et al.,

2003; Kondratenko and Kuperin, 2003; Stepanova et al., 2005; Lucio et al., 2007; Tao Cheng, 2008; Jiang et al., 2008; Sun et al., 2010; Ji and Chee, 2011; Wu and Chan, 2012; Zeng and Zhang, 2013; Benmahdjoub et al., 2013; Cheng et al., 2014). There are also hybrid approaches using time-delays and recurrent neural networks (see e.g. Kim, 1998).

The extension to spatial-temporal forecasting follows the same approach, i.e., using lags and an embedding dimension, but both in time and space. The approach results from merging this technique with another forecasting method unrelated to neural networks and described by Parlitz and Merkwirth (2000) for the reconstruction of spatial-temporal series. In their article they applied their approach successfully to both a spatial-temporal version of the Hénon map and to the Kuramoto-Sivashinsky non-linear equation. This method was later also applied with reasonable success to financial spatial-temporal series (interest rate curves) by Covas and Mena (2011) and to the sunspot butterfly diagram by Covas (2017), and by others to other data sets (Mandelj et al., 2001, 2004; Guo and Billings, 2007; Pan and Billings, 2008; Borštnik Bračić et al., 2009; Bialonski et al., 2015; Montañez and Shalizi, 2017). In these articles, a grid of inputs is build based on the two dimensional data series $s(n, m)$ to use in the search of the nearest neighbour in the embedding space, that once found, gives an approximation to the true future evolution in real physical space.

We shall describe our merged approach in detail in Section 2.1. Notice, however, that this is not the first time that neural networks have been applied to spatial-temporal forecasting (see e.g. French et al., 1992; Olligschlaeger and Gorr, 1997; Luk et al., 2000; Ganguly and Bras, 2002; Smaoui and Al-Enezi,

2004; Cheng and Wang, 2007; Tao Cheng, 2008; Sirvio and Hollmén, 2008; Qi and Li, 2009; Sauter et al., 2010; Wang et al., 2010; Wei et al., 2010). Nevertheless, we believe that this is the first time that neural networks have been applied to the problem of forecasting sunspots both in time and space (in this case latitude) and also, the first time that both the techniques of the first minima of the mutual information (for calculation of the optimum delays) and of the nearest false neighbours (for calculation of the embedding dimensions), belonging to the non-linear method, have been used to firmly define the architecture of the input layer of the neural network in both time and space within the overall purpose of forecasting. In both cases other articles restricted themselves to the temporal only problem.

2.1. Input layer architecture

There is no agreed universal prescription on how to setup a neural network input layer architecture (or other layers, for that matter). We have tried several approaches, i.e., several ways to slice the training set, and most of them did not work. Some reproduced the average spatial profile of the sunspots, some reproduced the temporal profile, while others simply failed to reproduce anything visually recognisable. Puzzled, we then tried using the way the spatial-temporal data is reconstructed for non-linear embeddings, as detailed on the sunspot forecasting article published by one of us (Covas, 2017). It turned out that this technique, known as the Parlitz-Merwirth method (Parlitz and Merkwirth, 2000), used to reconstruct local state data, when applied to the creation of the input patterns, immediately produced encouraging results. This input layer design can also be seen as a spatial-temporal generalization of the time delay neural network method (Waibel

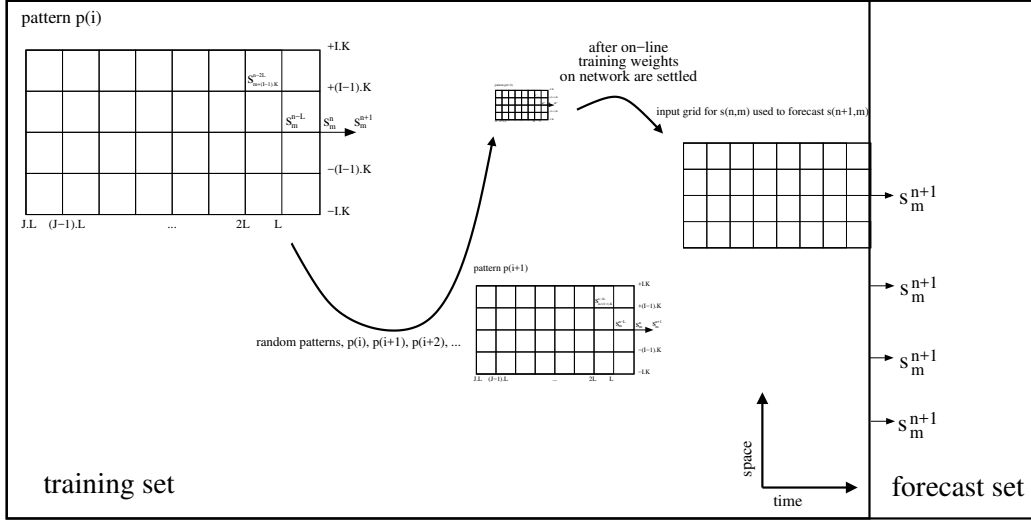


Figure 2: Forecasting method illustration. One constructs an embedding space using space and time delays, then assemble randomly positioned grid input patterns within the training set to pass to the neural network (in this figure we show 3 randomly selected input patterns). The input is a $(2I + 1)(J + 1)$ vector $\mathbf{x}(s_m^n)$ and the target (output) to train the network is the value s_m^{n+1} . After training with a sequence of patterns $p(i), p(i + 1), p(i + 2), \dots$ then the patterns adjacent to the forecast set are used to calculate the outputs to compare against the forecast. To forecast the $n + 2$ slice we concatenate the previously predicted $n + 1$ and progress accordingly.

et al., 1990; Luk et al., 2000; Frank et al., 2001; Oh and jae Kim, 2002; Sheng et al., 2003; Ghaderi et al., 2015). We shall now detail the Parlitz-Merwirth method when applied to the input layer architecture.

Let $n = 1, \dots, N$ and $m = 1, \dots, M$. Consider a spatial-temporal series s which can be defined by a $N \times M$ matrix with components $s_m^n \in \mathbb{R}$. To these components, we will call *states* of the spatial-temporal series. Consider a number $2I \in \mathbb{N}$ of neighbours in space of a given s_m^n and a number $J \in \mathbb{N}$ of temporal past neighbours relative to s_m^n (see Fig. 2). For each s_m^n , we define

the *super-state* vector $\mathbf{x}(s_m^n)$ with components given by s_m^n , its $2I$ spatial neighbours and its J past temporal neighbours, and with K and L being the spatial and temporal lags:

$$\mathbf{x}(s_m^n) = \{s_{m-IK}^n, \dots, s_m^n, \dots, s_{m+IK}^n, s_{m-IK}^{n-L}, \dots, s_m^{n-L}, \dots, s_{m+IK}^{n-L}, \dots, s_{m-IK}^{n-JL}, \dots, s_m^{n-JL}, \dots, s_{m+IK}^{n-JL}\} \quad (1)$$

So the dimension of each $\mathbf{x}(s_m^n)$ is

$$d = (2I + 1)(J + 1). \quad (2)$$

Notice that the embedding theorems by Whitney (1936), Takens (1981); Mañé (1981) and Sauer et al. (1991) do not express how to choose the space or time delays of the embedding¹. This can be done using the concept of *average mutual information* which has been used extensively in the past - see e.g. Fraser and Swinney (1986); Abarbanel (1997); Kantz and Schreiber (1997). Mutual information evaluates how measurements of s_j^i at time i are related to measurements of s_j^{i+L} at time $i + L$. This will give us an approximation for the values of the spatial and temporal delays K and L which can then be used to determining I and J and therefore the embedding dimension. After we calculate the (spatial and temporal) lags K and L , we can determine the embedding parameters I and J , for which we shall use the *method of false nearest neighbours* detection suggested by Kennel et al. (1992) and reported in detail in Martinerie et al. (1992); Abarbanel et al. (1993); Abarbanel and Gollub (1996); Abarbanel (1997). This approach determines

¹Notice there is also the possibility of instead of a global constant delay, to have an adaptive one (see e.g. Lin et al., 1992).

the number of neighbours of a point $\mathbf{x}(s_m^n)$ and how that number varies with growing embedding dimension. Below the theoretical or optimal embedding dimension, most of these neighbours will turn out to be false, only there due to projection effects, but at or on a larger embedding dimension we expect that all neighbours should be real. The advantage of adopting this auto-calibration as opposed to choosing those parameters based on the best match to the forecast or testing dataset is that we avert any bias. Using this approach the calibration is fully based on the training dataset and nothing else. These input vectors $\mathbf{x}(s_m^n)$ (in form of the nodes of a grid, see Fig. 2), are then passed as input to the neural network grid while the target (output) is s_m^{n+1} . Using this method, the number of input neurons is the same as the dimension of $\mathbf{x}(s_m^n)$, i.e., $(2I + 1)(J + 1)$. Although we do not know of any theoretical grounding for this approach, it seems reasonable to define the input layer architecture in this way, and after extensive searches, we found that this architecture, with its four auto-calibrated parameters, seems to be optimal for forecasting. The number of output neurons needed for this approach is just one, i.e. the forecasted s_m^{n+1} . Notice we could have adopted an output layer architecture identical to the input layer one, but we would end up with a series of multiple forecasts per observed spatial-temporal point, giving us a probabilistic forecast. For simplicity we decided to just use one forecast point, i.e., an output layer with one node only. Finally, the number of hidden nodes will be decided by trial and error later on, given that there seems to be no theoretically firm formula for the optimal number.

3. Results

3.1. The data

We use data for the sunspot area coverage² from 1874 to 2015. For later comparison, this is exactly the same data used in Covas (2017). The data we used starts at Carrington Rotation³ number 275 and finishes at 2162. The dataset is made of slices of 50 data points per Carrington Rotation, each point representing a bin in latitude, and these are distributed uniformly in $\sin(\text{latitude})$. The data points represent the area of that time/latitude “rectangle” that is covered by sunspot(s) in units of millionths of a hemisphere⁴. We take as a “training set” the data from the year 1874 to approximately 1997 (i.e. the first 1646 Carrington Rotations). We then attempt to reproduce or forecast the sunspot area butterfly diagram from Carrington Rotation 1921 to 2162 (the last one corresponding approximately to the year 2015); that is, we use 1646 time slices (~ 122.92 years) to reproduce the next 242 time slices (~ 18.07 years). The training set corresponds to around 12 solar cycles (cycle 11 to 22), while the “forecasting set” (or validation set) equates to around 1.5 cycles (cycle 23 and half of cycle 24). The entire dataset, including the training and forecasting sets, is a grid $A_j^i = A(i, j)$, with $i = 1888$ and $j = 50$. The training set is a grid $A(1646, 50)$. The sunspot area values, in units of

²We use the data set publicly available in <http://solarscience.msfc.nasa.gov/greenwch/bflydata.txt> (Hathaway, 2015a).

³Since the solar rotation at the surface varies with latitude and time, any method of analysing positions on the Sun’s surface over a period of time is inherently subjective. Solar rotation is taken to be 27.2752316 days. Each Sun’s rotation is given a unique number - the Carrington Rotation Number - starting from November 9, 1853.

⁴For details see <http://solar-b.msfc.nasa.gov/ssl/PAD/solar/greenwch.shtml>.

millionths of a hemisphere, range from 0 when there are no sunspots to the maximum value of around 2500.

3.2. Neural network parameter calibration

In a previous article (Covas, 2017) a calibration was made for the parameters I , J , K , L in equation (1) using the first minimum of the average mutual information for the K and L (spatial and temporal) lags and the false nearest neighbours method for finding the optimal embedding (spatial and temporal) dimensions I and J . The calibrated parameters for this training set were $I = 2$, $J = 6$, $K = 9$ and $L = 70$, i.e. following equation (2), each $\mathbf{x}(s_m^n)$ is made of $2 \times 2 + 1 = 5$ spatial neighbours times $6 + 1 = 7$ time delayed neighbours, with a spatial lag of 9 latitudinal slices and a temporal lag or delay of 70 Carrington rotations or time slices, corresponding to approximately 5.22 years. We shall use these choices of parameters to create training sets for the neural network and after the training, the input sets for the forecasts as depicted in Fig. 2. Notice that this calibration as done in Covas (2017) only depends on the training set, and therefore up to here, this approach is self-contained and auto-calibrated. Other parameters have to be decided empirically, as there is no agreed way to calculate them (see Stathakis, 2009, and references within). The most important is the number of hidden layers and the number of hidden neurons on each of those layers. The recommended number of layers depends on the problem at hand (Heaton, 2008; Stathakis, 2009). To keep the approach as simple as possible, we decided to use only one hidden layer. Regarding the number of hidden nodes N_h , there is again, as far as we know, no universally agreed procedure to decide what is the optimal number. Using too little will result in underfitting, and too many in

overfitting, or worst, in fitting the noise of the input data patterns. In our case, we have calculated the optimal number of hidden nodes by trial and error, as our particular case study does not require large computational power (an entire run with one million iterations takes a few minutes to complete on an average personal computer). We have seen that the neural network can produce realistic results when the number of nodes is between 50 and 100 or so, with an optimal value of $N_h = 70$ nodes. We shall use this value hereafter. We note that there are some algorithms, namely “pruning” and “constructive algorithms” (Cun et al., 1990; Hassibi and Stork, 1993; Reed and Marks II, 1999; Heaton, 2008) that try to overcome this problem, by starting with a large network and calculating which of the weights or links on the network are superfluous. For the purpose of this article, given that the data set is small, we will keep it as simple as possible and stay away from pruning and heuristic approaches and just do an exhaustive search. As for the back-propagation parameters η , α and ρ representing respectively the rate of learning, the momentum and the forgetfulness of the algorithm, we shall use, based on our searches, the values of $\eta = 0.3$, $\alpha = 0.01$ and $\rho = 0$. Notice we use a variation of the algorithm with an adaptive learning rate $\eta_n = \eta/(1 + n/10000)$, where η_n is the learning rate used at time step n . In addition to the depth and width of the hidden layer(s) architecture, another important degree of freedom is the choice of the activation function. Some authors (Han and Moraga, 1995) even consider different activation functions for the different layers. Here for simplicity we shall use the logistic or sigmoid function

$$F(x) = \frac{1}{1 + e^{-x}} \quad (3)$$

as the activation function for all layers. We tested other functions such as tanh and the log negative (see Reed and Marks II, 1999) but found the results disappointing. Another parametrization is what normalization to take (Reed and Marks II, 1999). In the case of the sunspots, we have area values from a minimum of 0 to a maximum of 2,580 in units of millionths of a hemisphere. One approach is to subtract the mean and divide by the standard deviation. However, the sunspot area distribution function does not follow a Gaussian distribution. In fact, the distribution is closer to a power law with an exponential cut-off, similar to the probability distribution function of the so called in-out intermittency (Ashwin et al., 1999). So, we take another approach, namely to apply the transformation:

$$x \rightarrow \alpha_{nor} + \frac{\ln(1+x)}{\beta_{nor}}, \quad (4)$$

where α_{nor} and β_{nor} are the arbitrary shift and scaling constants, respectively. Again, there is no clear rule on how to choose these and we calibrate them by trial and error. We have seen that the neural network can produce realistic results when the $\alpha_{nor} = 0$ and $\beta_{nor} = 10$. We shall use these values hereafter. Our final free set of parameters relates to the weights initialization. We choose random numbers with a constant distribution between $[0, 1]$ and shifted by α_{rng} and scaled by β_{rng} . We find that we obtain good results around $\alpha_{rng} = -0.5$ and $\beta_{rng} = 0.01$.

3.3. Training and forecast

In order to train the network, we have used one million iterations of different input patterns. Notice that the maximum number of different input patterns is $1646 \times 50 = 82,300$ patterns. However, for neural network training,

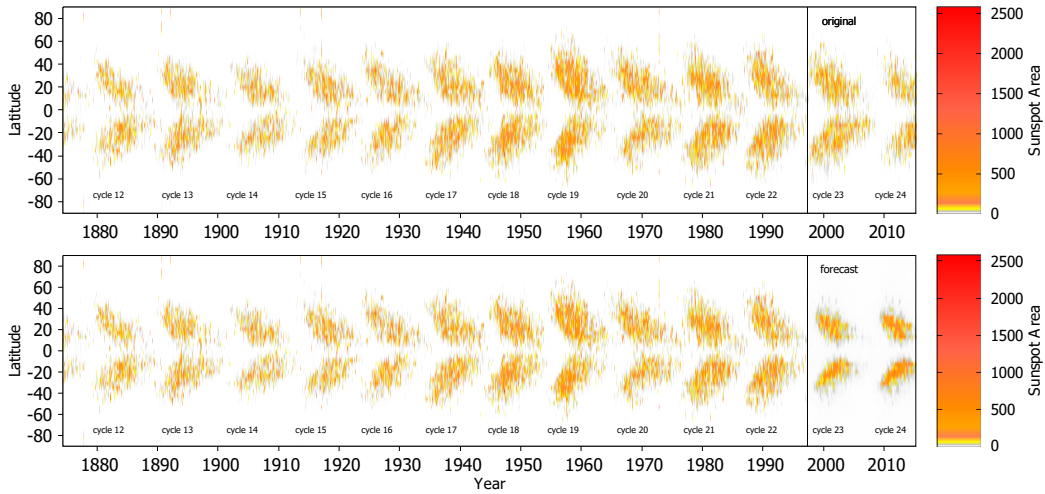


Figure 3: Spatial-temporal forecast of the last two cycles using the auto-calibrated parameters $I = 2$, $J = 6$, $K = 9$ and $L = 70$ and using the logistic or sigmoid function as the activation function, with $N_h = 70$ hidden nodes, and the free parameters $\eta = 0.3$, $\alpha = 0.01$, $\rho = 0$, $\alpha_{nor} = 0$, $\beta_{nor} = 10$, $\alpha_{rng} = -0.5$, $\beta_{rng} = 0.01$ with one million pattern iterations. The top panel is the full data set, including the training set and the actual observed future data. The bottom panel includes the training set plus the forecasted one. The division between the training set and the forecast set is depicted by a black line on both plots. Notice that the main characteristics of the sunspot butterfly diagram, particularly the amplitude of the cycle and the migration to the equator are both present, even if the reconstruction or forecast is far from perfect.

one randomly chooses patterns to optimize the weights, even if the number of iterations exceed the number of unique patterns, and using this approach is equivalent to a stochastic progress towards the minima of the error function (Reed and Marks II, 1999).

Using the best parameters calibration from section 3.2, we shall now attempt to forecast approximately 1.5 cycles (cycle 23 and half of cycle 24). We forecast one data slice at a time, i.e. one Carrington rotation at a time, then

concatenate the result to the training set, then use the same calibrated parameters to forecast the next and so on. A total of 242 data slices are forecast in this way. The results are depicted in Fig. 3. The results show that we can reproduce the two main features of the butterfly diagram, namely the amplitude shape of the cycle and the migration to the equator are both present, even if the forecast is far from perfect. There seems to be a concentration of points on the forecast and the butterfly wings look denser - still, overall, the qualitative aspects of the dynamics seem to be preserved by the forecast. To strengthen this conclusion, we also calculated the overall sunspot area (sum over latitude) for the forecast and compared it with the observed one. These results are depicted in Fig. 4. It shows the total sunspot area, both the original training set (and observed future set) and the forecasted set using the calibrated parameters. Although there is quite a lot of noise (on both sets), it shows that the method seems to qualitatively work not only in space and time but also on aggregated metrics such as the sum of the area over the latitude. This metric shows that the method is quite good at forecasting the first cycle (cycle 23) but, not surprisingly, starts to fail when forecasting the next cycle (cycle 24). This could indicate that the method can at most only forecast a few years ahead. Still the approach seems to be able to replicate quite well the entire shape of one whole cycle. We also calculate the sum over time, to show the average sunspot area as a function of latitude, another aggregated metric. This is shown in Fig. 5 and demonstrates that the method seems to be able to reproduce the real features in latitude as well as in time.

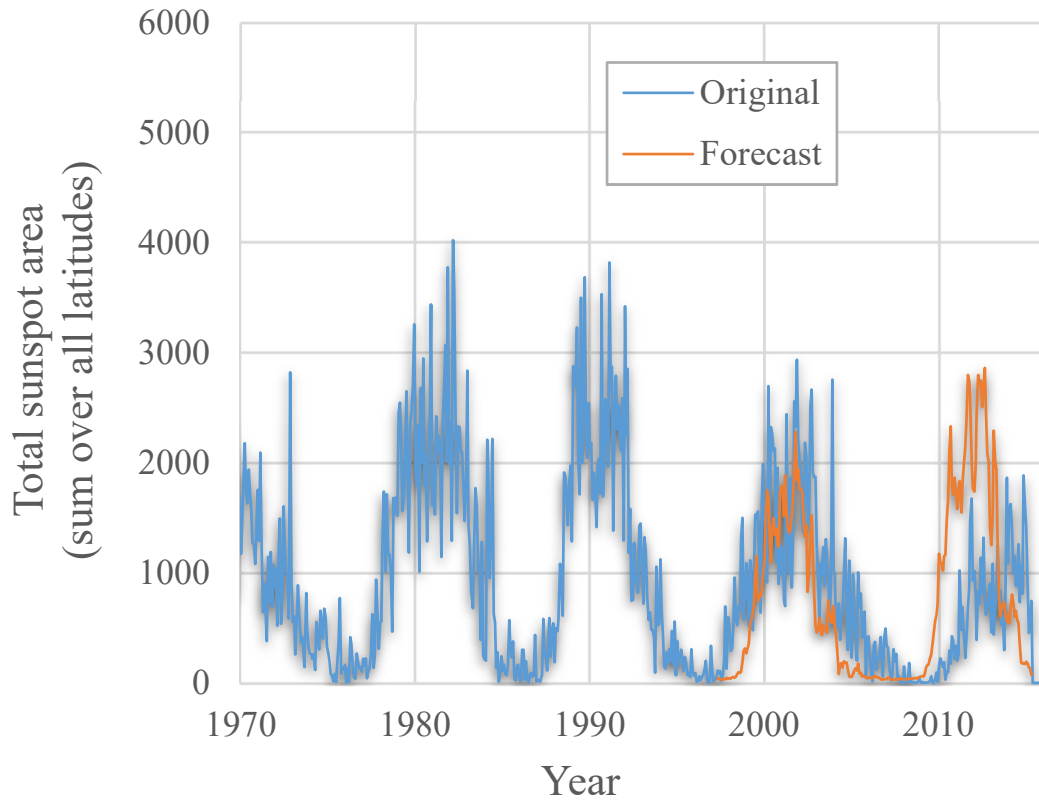


Figure 4: Overall sunspot area (sum over all latitudes) $A(t)$ and the forecast for the two last cycles (23 and 24) using the same parameters as in Fig. 3. The forecast for cycle 23 is reasonable but the method fails badly for cycle 24, showing clearly the limits of the approach at least in its current format.

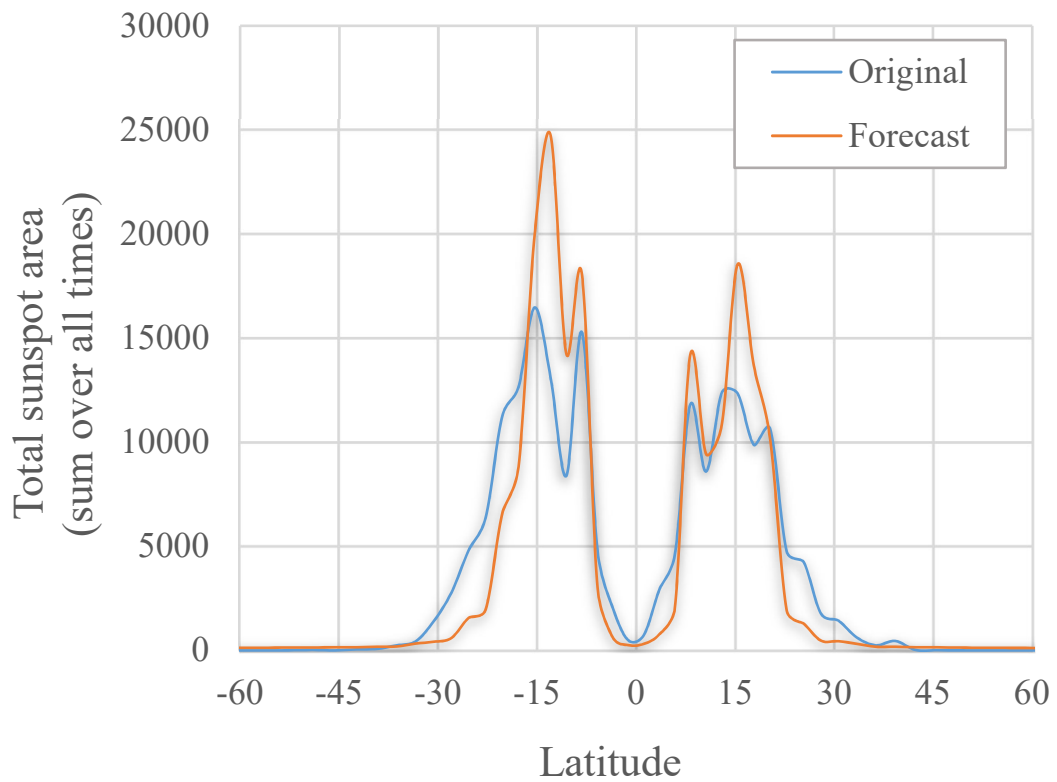


Figure 5: Overall sunspot area (sum over all times) $A(\theta)$ and the forecast for the two last cycles using the same parameters as in Fig. 3. The forecast gives a very similar latitudinal profile, with the two sunspot bands at mid-latitudes showing clearly on the plot.

3.4. Structural Similarity

The method used here has the advantage of forecasting the entire spatial-temporal features of the sunspot diagram. However, it is not easy to quantitatively verify that we have a good forecast. A human is able to look at the observed butterfly diagram and the predicted one in Fig. 3 and assess if it is a good or a bad forecast.

In order to evaluate the similarity of the prediction to the actual sunspot butterfly pattern we shall introduce the concept of structural similarity $SSIM(x, y)$ proposed by Wang et al. (2004) and used already in the context of sunspot forecasting in Covas (2017). For details on the technicalities of this measure see Wang et al. (2004); Brunet et al. (2012). The SSIM index is a numerical quantity used to calculate the perceived quality of digital images and videos. It allows two images to be compared and provides a value of their similarity. A value of $SSIM = 1$ corresponds to the case of two perfectly identical datasets or images. The SSIM index is designed to enhance on traditional methods such as the peak signal-to-noise ratio (PSNR) and the RMSE, which have proven (Wang and Bovik, 2009) to be inconsistent with human visual perception⁵. We shall use now the SSIM index to measure the similarity of the forecast and the original sunspot cycle. We verified that, as we randomly shift our neural network free parameters, for similar looking forecasts (as quantified by the human eye and the SSIM index), the RMSE value could oscillate widely. The underlying reason for the failure of the RMSE is that the butterfly diagram is not really a smooth two-dimensional surface, but a

⁵A particularly striking visual demonstration of the advantage of using SSIM over the RMSE index is show in <https://ece.uwaterloo.ca/~z70wang/research/ssim/#test>

very irregular dataset.

In section 3.3 we chose to split the full data set into a training set consisting of data up and including cycle 22 inclusive, with the remaining data, consisting of cycle 23 and the current cycle 24, being the forecasted set. We chose this split partly because we wanted to forecast at least one entire cycle, and partly because we wanted to do a consistent comparison with the previous results in Covas (2017). We should note, that due to the fact that the sunspot emergence and progression is cycle dependent (see e.g. Vitinskij, 1977; Li et al., 2001; Li et al., 2003; Hathaway et al., 2003; Solanki et al., 2008; Jiang et al., 2011; Ivanov and Miletsky, 2011) we should attempt to forecast other cycles as the actual effectiveness of the method in terms of actual predictability may vary cycle on cycle. The method depends only on the training set, and if a cycle, e.g. cycle 24, is relatively weak, then unless the training data has visited that rarely visited part of the supposedly underlying chaotic or strange attractor, the forecast will surely fail. The same presumably would apply for rare strong cycles. We also want to compare this method with the non-linear spatial-temporal embedding method in Covas (2017). To address both questions we ran an extra set of calculations going through all the cycles one by one and then attempted to predict cycle n using as the training set all cycles from the beginning of our dataset (cycle 11) to cycle $n - 1$. To decide when one cycle finishes and another starts, we used the data in Tables 1 and 2 in Hathaway (2015b), assuming that the beginning of each cycle corresponds to the minimum in the 13-month running mean. The results of this analysis are depicted in Fig. 6. First, we note that as the size of the training set increased, the predictive power of the method as

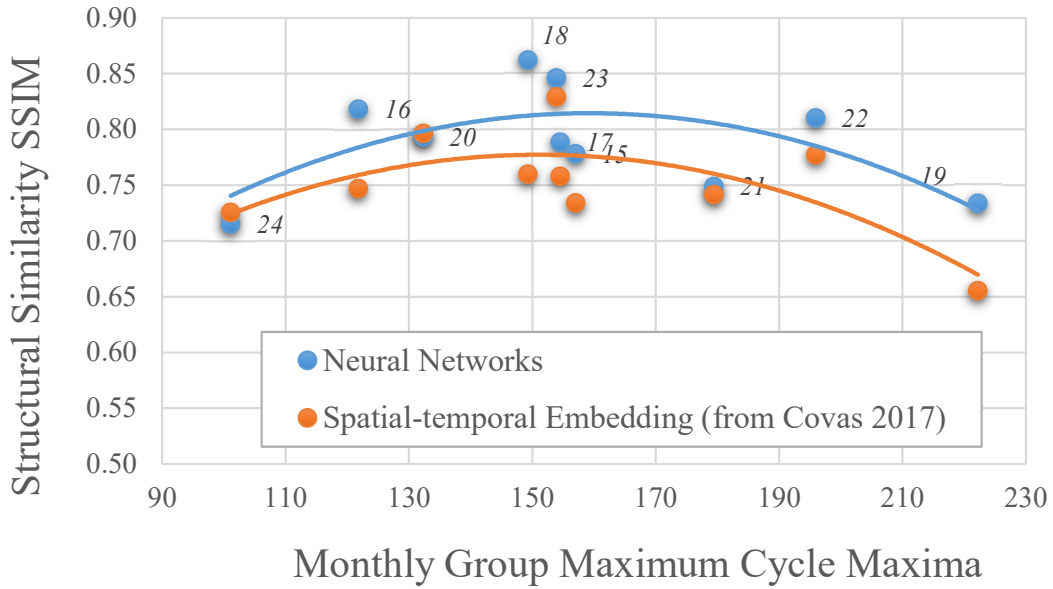


Figure 6: The structural similarity SSIM of the prediction set versus the original test set against the cycle strength as given by the Monthly Group Maximum sunspot number (Hathaway, 2015b). The plot labels represent the cycle number. The results show that the method is most effective for medium cycles. We did not include attempts to reconstruct cycles 11 to 14 (see Covas, 2017, for details). To increase the precision of the forecast, we took 20 million patterns per cycle, to compensate for the smaller average learning sets lengths than in the previous figures. We compared our results against Covas (2017) who used a spatial-temporal non-linear embedding approach. There is a clear similarity in both methods, both being less effective for weak and strong cycles. Overall, we observe that the neural networks approach has a small advantage over the spatial-temporal non-linear embedding approach.

measured by the SSIM index seemed to improve slightly. This is as expected, the larger the number of training patterns, the closer will the weights of the neural network be to the optimal asymptotic values. Second, the method described here seems to work better for medium cycles, as can be seen in the figure where we have superimposed a second-order polynomial fitting on the SSIM index versus the strength of the cycle. In particular, for the current cycle (as of end of 2017) - cycle 24, which is a weak cycle, the forecast is not that satisfactory. The neural network approach works on the basis of extracting knowledge from the training patterns. If there are not enough patterns tracing weak and strong cycles, then the weights will converge to values that tend to be biased towards medium cycles - the most common ones. Unless more data or extra features are added, it is difficult to improve the performance of this approach, a clear limitation of just using sunspot data rather than all related physical data. Some authors argue that one should use further physical data, e.g. geomagnetic precursors (Feynman, 1982; Schatten and Sofia, 1987; Thompson, 1993; Hathaway et al., 1999; Hathaway and Wilson, 2006; Kane, 2007; Cameron and Schüssler, 2007; Wang and Sheeley, 2009; Ng, 2016); surface magnetic fields, in particular polar fields (Schatten et al., 1978; Svalgaard et al., 2005; Muñoz-Jaramillo et al., 2013a; Petrie et al., 2014); polar faculae (Muñoz-Jaramillo et al., 2012, 2013b); and even helioseismological data (Ilonidis et al., 2011, 2013). Nevertheless, it is outside the scope of this article to include further data. We note, however, that the neural networks approach allows the inclusion of other data easily, even if these are just pure time series with no spatial component, as long as the temporal number and frequency of data points is the same as the sunspot data. We plan to pursue

this research avenue in a forthcoming article. Here we have limited ourselves to demonstrating the possibility of qualitatively forecast using a pure statistical model, i.e., another approach to be added to the existing ones in the literature, such as ones that use empirical relationships (Jiang et al., 2011; Santos et al., 2015; Cameron et al., 2016) or the magnetic field data (McIntosh et al., 2014; McIntosh et al., 2014; Jiang and Cao, 2017). Third and finally Fig. 6 shows that the neural network method performs slightly better than the non-linear spatial-temporal embedding approach in Covas (2017). This is quite encouraging.

Finally, one can ask how far ahead can any approach realistically forecast. The answer depends on whether the modulation, i.e., the variations in the period and amplitude of the solar cycle, is a result of a chaotic attractor or simply a stochastic fluctuation on top of a basic cycle. Although the time series we have seem quite long (from 1874 to today), in a statistical sense it is not long enough to clarify what is the answer to the question above. However, we believe that our method, even if it assumes the existence of a chaotic attractor, can recreate qualitatively most of features of the spatially extended solar cycle and that this is suggestive that perhaps the solar cycle can be modelled by a weakly chaotic attractor. Some researchers have attempted to answer this question using different numerical methods (Carbonell et al., 1993, 1994; Hanslmeier and Brajša, 2010; Love and Rigler, 2012; Hanslmeier et al., 2013; Zhou et al., 2014), but again, given the size of the data set (in time), it seems to indicate that for now we cannot be sure which hypothesis, a chaotic attractor or a stochastic modulation superimposed on a periodic component, is the true one. Other authors have argued that even

if the attractor exists, it is fundamentally unpredictable (Bushby and Tobias, 2007).

4. Conclusion

We used the so-called feedforward artificial neural networks in an attempt to forecast the sunspot butterfly diagram in both space and time. As far as we aware, this is the first time this has been attempted using neural networks - all the work in the literature focus on using neural networks applied to pure sunspot temporal metrics, such as the average sunspot number or sunspot area time series. To contrast, here we attempt to use neural networks to predict sunspots both in time and space.

The results show that even though the method can reproduce qualitatively some of the main features of the sunspot diagram, such as the overall cycle amplitude modulation, and the cycle's sunspot migration to the equator, it does not seem to have a real predictive power, at least in its current format. This is clearly demonstrated in the analysis of the structure similarity index against the cycle's strength, which shows that the method has a bias towards average cycles. This is consistent on what was seen when using a non-linear embedding method in Covas (2017). In fact, there seems to be quite a parallel in the results of the two forecasting methods.

We also found that the spatial-temporal non-linear embedding method in Parlitz and Merkwirth (2000) points the way for the optimal input layer architecture, an empirical result that may show there is some general-purpose theorem waiting to be demonstrated.

We believe that the work points in the right direction, first that we ought

to attempt to forecast in space as well as in time, and second that further improvements ought to be tried. The first improvement must surely be to use recurrent networks, such as Elman networks (Elman, 1990) which are known to be more appropriate to model time series (although more complex to design and construct). The second improvement that we suggest is to incorporate related information as additional input(s), e.g., to use solar magnetic field proxies such as the 10.7cm radio flux and the 530.3nm green coronal index (Broomhall and Nakariakov, 2015) and even geomagnetic proxies such as the *aa* indices (Mayaud, 1972; Nevanlinna and Kataja, 1993). In this article we wanted to focus on showing that neural networks can qualitatively model both the spatial and the temporal dynamics of the sunspot diagram and we plan to revisit the improvements mentioned above in future work.

Further to sunspots, it ought to be worthwhile to explore predicting other physically related spatial-temporal data series such as the ones depicting the vertical magnetic flux through the solar photosphere. This data series goes back only to 1975 but has a very high resolution and in contrast to sunspot data, is a smoother data set, so it should be a promising research area to work on. Also, the data series representing bright spots in the Sun, which are called active region faculae, is also available and one should pursue using it as well to compare with the sunspot analysis done here, as both sunspots and faculae are correlated with strong magnetic fields at the solar surface and are associated with driving space weather. Predicting the second order variation of the Sun's surface rotation rate in latitude and time, known as torsional oscillations, which shows a similar pattern to the sunspot diagram,

could also be used as input for these forecasting methods.

Overall we think the forecasting in higher dimensions, even if it is harder computationally and more demanding in terms of data samples, should open many research avenues within solar physics and within the area of space weather science.

Acknowledgements

We would like to thank Reza Tavakol for very useful discussions on sunspot forecasting. We also thank Dr. David Hathaway for providing the data that this article is based upon. N. Peixinho acknowledges funding by the Portuguese FCT - Foundation for Science and Technology and the European Social Fund (ref: SFRH/BGCT/113686/2015). CITEUC is funded by National Funds through FCT - Foundation for Science and Technology (project: UID/Multi/00611/2013) and FEDER - European Regional Development Fund through COMPETE 2020 - Operational Programme Competitiveness and Internationalization (project: POCI-01-0145-FEDER-006922).

References

- Abarbanel, H., 1997. Analysis of Observed Chaotic Data. Institute for Non-linear Science. Springer New York.
- Abarbanel, H. D. I., Brown, R., Sidorowich, J. J., Tsimring, L. S., Oct. 1993. The analysis of observed chaotic data in physical systems. *Reviews of Modern Physics* 65, 1331–1392.
- Abarbanel, H. D. I., Gollub, J. P., Nov. 1996. Analysis of Observed Chaotic Data. *Physics Today* 49, 86.

- Abreu, J. A., Beer, J., Ferriz-Mas, A., McCracken, K. G., Steinhilber, F.,
Dec. 2012. Is there a planetary influence on solar activity? *A&A*548, A88.
- Acero, F. J., Carrasco, V. M. S., Gallego, M. C., García, J. A., Vaquero,
J. M., Apr. 2017. Extreme Value Theory and the New Sunspot Number
Series. *ApJ*839, 98.
- Ajabshirizadeh, A., Juzdani Nafiseh, M., 2010. Sunspot Number and So-
lar Radio Flux Prediction by Artificial Neural Network Method. In: 38th
COSPAR Scientific Assembly. Vol. 38 of COSPAR Meeting. p. 2.
- Ajabshirizadeh, A., Masoumzadeh Jouzdani, N., Abbassi, S., Apr. 2011. Neu-
ral network prediction of solar cycle 24. *Research in Astronomy and As-
trophysics* 11, 491–496.
- Annunziato, M., Pizzuti, S., Tsimring, L. S., 2000. Analysis and prediction
of spatio-temporal flame dynamics. In: Setti, G., Rovatti, R., Mazzini,
G. (Eds.), *Proceedings of the IEEE Workshop on Nonlinear Dynamics of
Electronic Systems: Catania, Italy, 18-20 May 2000*. World Scientific, pp.
117–121.
- Ashwin, P., Covas, E., Tavakol, R., May 1999. Transverse instability for
non-normal parameters. *Nonlinearity* 12, 563–577.
- Attia, A.-F., Abdel-Hamid, R., Quassim, M., Mar. 2005. Prediction of Solar
Activity Based on Neuro-Fuzzy Modeling. *Sol. Phys.*227, 177–191.
- Attia, A.-F., Ismail, H. A., Basurah, H. M., Mar. 2013. A Neuro-Fuzzy mod-
eling for prediction of solar cycles 24 and 25. *Ap&SS*344, 5–11.

- Attia, A.-F. A., Abdel-Hamid, R. H., Quassim, M., Sep. 2004. A genetic-based neuro-fuzzy approach for prediction of solar activity. In: Craig, S. C., Cullum, M. J. (Eds.), *Modeling and Systems Engineering for Astronomy*. Vol. 5497 of Proc. SPIE. pp. 542–552.
- Beer, J., Tobias, S., Weiss, N., Jul. 1998. An Active Sun Throughout the Maunder Minimum. *Sol. Phys.*181, 237–249.
- Benmahdjoub, K., Ameer, Z., Boulifa, M., 2013. Forecasting of rainfall using time delay neural network in tizi-ouzou (algeria). *Energy Procedia* 36, 1138 – 1146.
- Bialonski, S., Ansmann, G., Kantz, H., Oct 2015. Data-driven prediction and prevention of extreme events in a spatially extended excitable system. *Phys. Rev. E* 92, 042910.
- Borštnik Bračić, A., Grabec, I., Govekar, E., 2009. Modeling spatio-temporal field evolution. *The European Physical Journal B* 69 (4), 529–538.
- Box, G. E. P., Jenkins, G. M. (Eds.), 1976. *Time series analysis. Forecasting and control*.
- Broomhall, A.-M., Nakariakov, V. M., Nov. 2015. A Comparison Between Global Proxies of the Sun’s Magnetic Activity Cycle: Inferences from Helioseismology. *Sol. Phys.*290, 3095–3111.
- Brunet, D., Vrscay, E. R., Wang, Z., Apr. 2012. On the Mathematical Properties of the Structural Similarity Index. *IEEE Transactions on Image Processing* 21, 1488–1499.

- Bushby, P. J., Tobias, S. M., Jun. 2007. On Predicting the Solar Cycle Using Mean-Field Models. *ApJ*661, 1289–1296.
- Calvo, R. A., Ceccato, H. A., Piacentini, R. D., May 1995. Neural network prediction of solar activity. *ApJ*444, 916–921.
- Cameron, R., Schüssler, M., Apr. 2007. Solar Cycle Prediction Using Precursors and Flux Transport Models. *ApJ*659, 801–811.
- Cameron, R. H., Jiang, J., Schüssler, M., Jun. 2016. Solar Cycle 25: Another Moderate Cycle? *ApJ*823, L22.
- Carbonell, M., Oliver, R., Ballester, J. L., Jul. 1993. On the asymmetry of solar activity. *A&A*274, 497.
- Carbonell, M., Oliver, R., Ballester, J. L., Oct. 1994. A search for chaotic behaviour in solar activity. *A&A*290, 983–994.
- Cass, D., Shell, K., 1983. Do sunspots matter? *Journal of Political Economy* 91 (2), 193–227.
- Chandra, R., Zhang, M., Jun. 2012. Cooperative coevolution of elman recurrent neural networks for chaotic time series prediction. *Neurocomput.* 86, 116–123.
- Charbonneau, P., Jan. 2013. Solar physics: The planetary hypothesis revived. *Nature*493, 613–614.
- Chattopadhyay, G., Chattopadhyay, S., Apr. 2012. Monthly sunspot number time series analysis and its modeling through autoregressive artificial neural network. *European Physical Journal Plus* 127, 43.

- Chattopadhyay, S., Jhajharia, D., Chattopadhyay, G., Jul. 2011. Trend estimation and univariate forecast of the sunspot numbers: Development and comparison of ARMA, ARIMA and Autoregressive Neural Network models. *Comptes Rendus Geoscience* 343, 433–442.
- Cheng, T., Wang, J., 2007. Application of a dynamic recurrent neural network in spatio-temporal forecasting. In: *Information Fusion and Geographic Information Systems*. Springer, pp. 173–186.
- Cheng, T., Wang, J., Haworth, J., Heydecker, B., Chow, A., 2014. A dynamic spatial weight matrix and localized spacetime autoregressive integrated moving average for network modeling. *Geographical Analysis* 46 (1), 75–97.
- Conway, A., 1994. Echoed time series predictions, neural networks and genetic algorithms. *Vistas in Astronomy* 38, 351–356.
- Conway, A. J., Oct. 1998. Time series, neural networks and the future of the Sun. *New A Rev.*42, 343–394.
- Conway, A. J., Macpherson, K. P., Blacklaw, G., Brown, J. C., Dec. 1998. A neural network prediction of solar cycle 23. *J. Geophys. Res.*103, 29733–29742.
- Covas, E., Sep. 2017. Spatial-temporal forecasting the sunspot diagram. *A&A*605, A44.
- Covas, E., Mena, F., 2011. Forecasting of yield curves using local state space reconstruction. In: Peixoto, M. M., Pinto, A. A., Rand, D. A. (Eds.),

- Dynamics, Games and Science I. Vol. 1 of Springer Proceedings in Mathematics. Springer Berlin Heidelberg, pp. 243–251.
- Cun, Y. L., Denker, J. S., Solla, S. A., 1990. In: Touretzky, D. S. (Ed.), *Advances in Neural Information Processing Systems 2*. Morgan Kaufmann Publishers Inc., San Francisco, CA, USA, Ch. Optimal Brain Damage, pp. 598–605.
- Dikpati, M., de Toma, G., Gilman, P. A., Mar. 2006. Predicting the strength of solar cycle 24 using a flux-transport dynamo-based tool. *Geophys. Res. Lett.*33, L05102.
- Ding, L., Lan, R., Jiang, Y., Peng, J., 2012. Prediction of the smoothed monthly mean sunspot area based on neural network. *Transactions of Atmospheric Sciences* 4, 015.
- Duhau, S., Mar. 2003. An Early Prediction of Maximum Sunspot Number in Solar Cycle 24. *Sol. Phys.*213, 203–212.
- Elman, J. L., 1990. Finding structure in time. *Cognitive Science* 14 (2), 179–211.
- Elshorbagy, A., Simonovic, S. P., Panu, U. S., Jan. 2002. Estimation of missing streamflow data using principles of chaos theory. *Journal of Hydrology* 255, 123–133.
- Emmert-Streib, F., Dehmer, M., 2007. Nonlinear Time Series Prediction Based on a Power-Law Noise Model. *International Journal of Modern Physics C* 18, 1839–1852.

- Fessant, F., Bengio, S., Collobert, D., Jan. 1996a. On the prediction of solar activity using different neural network models. *Annales Geophysicae* 14, 20–26.
- Fessant, F., Pierret, C., Lantos, P., Oct. 1996b. Comparison of Neural Network and McNish and Lincoln Methods for the Prediction of the Smoothed Sunspot Index. *Sol. Phys.*168, 423–433.
- Feynman, J., Aug. 1982. Geomagnetic and solar wind cycles, 1900-1975. *J. Geophys. Res.*87, 6153–6162.
- Francile, C., Luoni, M. L., 2010. Hacia la predicción del Número R de Wolf de manchas solares utilizando Redes Neuronales con retardos temporales. *Boletín de la Asociación Argentina de Astronomía La Plata Argentina* 53, 241–244.
- Frank, R. J., Davey, N., Hunt, S. P., 2001. Time series prediction and neural networks. *Journal of Intelligent and Robotic Systems* 31 (1), 91–103.
- Fraser, A. M., Swinney, H. L., Feb. 1986. Independent coordinates for strange attractors from mutual information. *Phys. Rev. A* 33, 1134–1140.
- French, M. N., Krajewski, W. F., Cuykendall, R. R., 1992. Rainfall forecasting in space and time using a neural network. *Journal of hydrology* 137 (1-4), 1–31.
- Gang, D., Shi-Sheng, Z., 2007. Sunspot number prediction based on process neural network with time-varying threshold functions [j]. *Acta Physica Sinica* 2, 099.

- Ganguly, A., Bras, R., 2002. Artificial neural networks and ensemble techniques for space time forecasting of mean and confidence bounds over multiple leads. In: AGU Spring Meeting Abstracts.
- Ghaderi, A. H., Bharani, B., Jalalkamali, H., 2015. Embedding dimension as input dimension of artificial neural network: A study on stock prices time series. *International Journal of Modern Physics and Applications* 1 (3), 64–72.
- Gholipour, A., Lucas, C., Araabi, B. N., Shafiee, M., Apr. 2005. Solar activity forecast: Spectral analysis and neurofuzzy prediction. *Journal of Atmospheric and Solar-Terrestrial Physics* 67, 595–603.
- Gkana, A., Zachilas, L., 2015. Sunspot numbers: Data analysis, predictions and economic impacts. *Journal of Engineering Science and Technology Review* 8 (1), 79–85, cited By 1.
- Guo, L., Billings, S. A., 2007. State-space reconstruction and spatio-temporal prediction of lattice dynamical systems. *IEEE Transactions on Automatic Control* 52 (4), 622–632.
- Hale, G. E., Nov. 1908. On the Probable Existence of a Magnetic Field in Sun-Spots. *ApJ*28, 315.
- Han, J., Moraga, C., 1995. The influence of the sigmoid function parameters on the speed of backpropagation learning. Springer Berlin Heidelberg, Berlin, Heidelberg, pp. 195–201.
- Han, M., Xi, J., Xu, S., Yin, F.-L., 2004. Prediction of chaotic time series

- based on the recurrent predictor neural network. *IEEE Transactions on signal processing* 52 (12), 3409–3416.
- Hanslmeier, A., Brajša, R., Jan. 2010. The chaotic solar cycle. I. Analysis of cosmogenic ^{14}C -data. *A&A*509, A5.
- Hanslmeier, A., Brajša, R., Čalogović, J., Vršnak, B., Ruždjak, D., Steinhilber, F., MacLeod, C. L., Ivezić, Ž., Skokić, I., Feb. 2013. The chaotic solar cycle. II. Analysis of cosmogenic ^{10}Be data. *A&A*550, A6.
- Hassibi, B., Stork, D. G., 1993. Second order derivatives for network pruning: Optimal brain surgeon. In: *Advances in Neural Information Processing Systems* 5, [NIPS Conference]. Morgan Kaufmann Publishers Inc., San Francisco, CA, USA, pp. 164–171.
- Hathaway, D. H., feb 2015a. Sunspot Area Butterfly Diagram data.
URL <http://solarscience.msfc.nasa.gov/greenwch.shtml>
- Hathaway, D. H., Sep. 2015b. The Solar Cycle. *Living Reviews in Solar Physics* 12.
- Hathaway, D. H., Nandy, D., Wilson, R. M., Reichmann, E. J., May 2003. Evidence That a Deep Meridional Flow Sets the Sunspot Cycle Period. *ApJ*589, 665–670.
- Hathaway, D. H., Wilson, R. M., Sep. 2006. Geomagnetic activity indicates large amplitude for sunspot cycle 24. *Geophys. Res. Lett.*33, L18101.
- Hathaway, D. H., Wilson, R. M., Reichmann, E. J., Oct. 1999. A Synthesis of Solar Cycle Prediction Techniques. *J. Geophys. Res.*104, 22.

- Heaton, J., 2008. Introduction to Neural Networks for Java, 2Nd Edition, 2nd Edition. Heaton Research, Inc.
- Ilonidis, S., Zhao, J., Hartlep, T., Nov. 2013. Helioseismic Investigation of Emerging Magnetic Flux in the Solar Convection Zone. *ApJ*777, 138.
- Ilonidis, S., Zhao, J., Kosovichev, A., Aug. 2011. Detection of Emerging Sunspot Regions in the Solar Interior. *Science* 333, 993.
- Ivanov, V. G., Miletsky, E. V., Jan. 2011. Width of Sunspot Generating Zone and Reconstruction of Butterfly. *Sol. Phys.*268, 231–242.
- Ji, W., Chee, K. C., 2011. Prediction of hourly solar radiation using a novel hybrid model of arma and tdnn. *Solar Energy* 85 (5), 808–817.
- Jiang, C., Song, F., 2011. Sunspot forecasting by using chaotic time-series analysis and narx network. *JCP* 6 (7), 1424–1429.
- Jiang, J., Cameron, R. H., Schmitt, D., Schüssler, M., Apr. 2011. The solar magnetic field since 1700. I. Characteristics of sunspot group emergence and reconstruction of the butterfly diagram. *A&A*528, A82.
- Jiang, J., Cao, J., Jul. 2017. Predicting solar surface large-scale magnetic field of Cycle 24. ArXiv e-prints.
- Jiang, W., Zhang, L., Wang, P., 2008. Nonlinear time series forecasting of time-delay neural network embedded with bayesian regularization. *Applied Mathematics and Computation* 205 (1), 123 – 132, special Issue on Life System Modeling and Bio-Inspired Computing for {LSMS} 2007.

- Kaastra, I., Boyd, M., 1996. Designing a neural network for forecasting financial and economic time series. *Neurocomputing* 10 (3), 215 – 236, financial Applications, Part {II}.
- Kane, R. P., Oct. 1999. Prediction of the sunspot maximum of solar cycle 23 by extrapolation of spectral components. *Sol. Phys.*189, 217–224.
- Kane, R. P., Jul. 2007. A Preliminary Estimate of the Size of the Coming Solar Cycle 24, based on Ohl’s Precursor Method. *Sol. Phys.*243, 205–217.
- Kantz, H., Schreiber, T., 1997. *Nonlinear time series analysis*. Cambridge nonlinear science series. Cambridge University Press, Cambridge, New York, originally published: 1997.
- Kennel, M. B., Brown, R., Abarbanel, H. D. I., Mar. 1992. Determining embedding dimension for phase-space reconstruction using a geometrical construction. *Phys. Rev. A*45, 3403–3411.
- Kim, H., Eykholt, R., Salas, J., 1999. Nonlinear dynamics, delay times, and embedding windows. *Physica D: Nonlinear Phenomena* 127 (12), 48 – 60.
- Kim, S.-S., 1998. Time-delay recurrent neural network for temporal correlations and prediction. *Neurocomputing* 20 (1), 253–263.
- Kim, T.-H., Park, D.-C., Woo, D.-M., Huh, W., Yoon, C.-H., Kim, H.-U., Lee, Y., 2010. Sunspot series prediction using a multiscale recurrent neural network. In: *Signal Processing and Information Technology (ISSPIT)*, 2010 IEEE International Symposium on. IEEE, pp. 399–403.

- Kondratenko, V. V., Kuperin, Y. A., 2003. Using recurrent neural networks to forecasting of forex. Papers, arXiv.org.
- Koons, H. C., Gorney, D. J., May 1990. A sunspot maximum prediction using a neural network. EOS Transactions 71, 677.
- Kornblueh, I. H., Feb. 1965. In memoriam Alexander Leonidovich Tchijevsky. International Journal of Biometeorology 9, 99–99.
- Koskela, T., Lehtokangas, M., Saarinen, J., Kaski, K., 1996. Time series prediction with multilayer perceptron, fir and elman neural networks. In: In Proceedings of the World Congress on Neural Networks. Press, pp. 491–496.
- Krizhevsky, A., Sutskever, I., Hinton, G. E., 2012. Imagenet classification with deep convolutional neural networks. In: Advances in Neural Information Processing Systems. pp. 1097–1105.
- Kulkarni, D. R., Pandya, A. S., Parikh, J. C., 1998. Modeling and predicting sunspot activity-state space reconstruction + artificial neural network methods. Geophys. Res. Lett.25, 457–460.
- Kulkarni, D. R., Parikh, J. C., Pandya, A. S., 1997. Dynamic Predictions from Time Series Data - An Artificial Neural Network Approach. International Journal of Modern Physics C 8, 1345–1360.
- Lecun, Y., Bottou, L., Bengio, Y., Haffner, P., 1998. Gradient-based learning applied to document recognition. In: Proceedings of the IEEE. pp. 2278–2324.

- Leung, H., Lo, T., Jul. 1993. Chaotic radar signal processing over the sea. *IEEE Journal of Oceanic Engineering* 18, 287–295.
- Li, G., Wang, S., 01 2017. Sunspots time-series prediction based on complementary ensemble empirical mode decomposition and wavelet neural network. *Mathematical Problems in Engineering* 2017, 1–7.
- Li, K., Wang, J., Zhan, L., Yun, H., Liang, H., Zhao, H., Gu, X., 2003. On the latitudinal distribution of sunspot groups over a solar cycle. *Solar Physics* 215 (1), 99–109.
- Li, K. J., Yun, H. S., Gu, X. M., Oct. 2001. Latitude Migration of Sunspot Groups. *AJ122*, 2115–2117.
- Li, M., Mehrotra, K., Mohan, C., Ranka, S., Sep 1990. Sunspot numbers forecasting using neural networks. In: *Proceedings. 5th IEEE International Symposium on Intelligent Control* 1990. pp. 524–529 vol.1.
- Lin, D.-T., Dayhoff, J. E., Ligomenides, P. A., 1992. Adaptive time-delay neural network for temporal correlation and prediction. In: *Applications in Optical Science and Engineering. International Society for Optics and Photonics*, pp. 170–181.
- Liu, Z.-G., Du, J., 2012. Sunspot time sequences prediction based on process neural network and quantum particle swarm. In: *Multimedia Information Networking and Security (MINES), 2012 Fourth International Conference on. IEEE*, pp. 233–236.
- Love, J. J., Rigler, E. J., May 2012. Sunspot random walk and 22-year variation. *Geophys. Res. Lett.*39, L10103.

- Lucio, P. S., Conde, F. C., Cavalcanti, I. F. A., Serrano, A. I., Ramos, A. M., Cardoso, A. O., Apr. 2007. Spatiotemporal monthly rainfall reconstruction via artificial neural network - case study: south of Brazil. *Advances in Geosciences* 10, 67–76.
- Luk, K., Ball, J. E., Sharma, A., 2000. A study of optimal model lag and spatial inputs to artificial neural network for rainfall forecasting. *Journal of Hydrology* 227 (1), 56–65.
- Lundstedt, H., 2001. Solar activity predicted with artificial intelligence. Washington DC American Geophysical Union Geophysical Monograph Series 125, 201–204.
- Lundstedt, H., Wik, M., Wintoft, P., Dec. 2006. Synoptic Solar Magnetic Fields: Explored and Predicted. AGU Fall Meeting Abstracts.
- Luthardt, L., Röbber, R., Mar. 2017. Fossil forest reveals sunspot activity in the early Permian. *Geology* 45, 279–282.
- Mañé, R., 1981. On the dimension of the compact invariant sets of certain non-linear maps. *Lecture Notes in Mathematics*, Berlin Springer Verlag 898, 230.
- MacPherson, K., Sep. 1993. Neural network computation techniques applied to solar activity prediction. *Advances in Space Research* 13, 447–450.
- Macpherson, K. P., Conway, A. J., Brown, J. C., Nov. 1995. Prediction of solar and geomagnetic activity data using neural networks. *J. Geophys. Res.*100, 21735–21744.

- Mandelj, S., Grabec, I., Govekar, E., 2001. Statistical approach to modeling of spatiotemporal dynamics. *International Journal of Bifurcation and Chaos* 11 (11), 2731–2738.
- Mandelj, S., Grabec, I., Govekar, E., 2004. Nonparametric statistical modeling of spatiotemporal dynamics based on recorded data. *International Journal of Bifurcation and Chaos* 14 (06), 2011–2025.
- Maris, G., Oncica, A., Mar. 2006. Solar Cycle 24 Forecasts. *Sun and Geosphere* 1 (1), 8–11.
- Martinerie, J. M., Albano, A. M., Mees, A. I., Rapp, P. E., May 1992. Mutual information, strange attractors, and the optimal estimation of dimension. *Phys. Rev. A* 45, 7058–7064.
- Maslennikova, Y., Bochkarev, V., Jul. 2012. Solar activity prediction using artificial neural network and singular spectrum analysis. In: 39th COSPAR Scientific Assembly. Vol. 39 of COSPAR Meeting. p. 1194.
- Maslennikova, Y. S., Bochkarev, V. V., 2014. Training algorithm for neuro-fuzzy network based on singular spectrum analysis. *CoRR* abs/1410.1151.
- Mayaud, P.-N., 1972. The aa indices: A 100-year series characterizing the magnetic activity. *J. Geophys. Res.* 77, 6870.
- McIntosh, S. W., Wang, X., Leamon, R. J., Davey, A. R., Howe, R., Krista, L. D., Malanushenko, A. V., Markel, R. S., Cirtain, J. W., Gurman, J. B., Pesnell, W. D., Thompson, M. J., 2014. Deciphering solar magnetic activity. i. on the relationship between the sunspot cycle and the evolution of small magnetic features. *The Astrophysical Journal* 792 (1), 12.

- McIntosh, S. W., Wang, X., Leamon, R. J., Scherrer, P. H., Apr. 2014. Identifying Potential Markers of the Sun's Giant Convective Scale. *ApJ*784, L32.
- Mirmomeni, M., Shafiee, M., Lucas, C., Araabi, B. N., Dec. 2006. Introducing a new learning method for fuzzy descriptor systems with the aid of spectral analysis to forecast solar activity. *Journal of Atmospheric and Solar-Terrestrial Physics* 68, 2061–2074.
- Moghaddam, J. D., Mosallanezhad, A., Teshnehlab, M., 2013. Sunspot prediction by a time delay line recurrent fuzzy neural network using emotional learning. In: *Fuzzy Systems (IFSC), 2013 13th Iranian Conference on*. IEEE, pp. 1–5.
- Montañez, G. D., Shalizi, C. R., May 2017. The licors cabinet: Nonparametric light cone methods for spatio-temporal modeling. In: *2017 International Joint Conference on Neural Networks (IJCNN)*. pp. 2811–2819.
- Mordvinov, A. V., Makarenko, N. G., Ogurtsov, M. G., Jungner, H., Oct. 2004. Reconstruction of Magnetic Activity of the Sun and Changes in Its Irradiance on a Millennium Timescale Using Neurocomputing. *Sol. Phys.*224, 247–253.
- Muñoz-Jaramillo, A., Balmaceda, L. A., DeLuca, E. E., Jul. 2013a. Using the Dipolar and Quadrupolar Moments to Improve Solar-Cycle Predictions Based on the Polar Magnetic Fields. *Physical Review Letters* 111 (4), 041106.

- Muñoz-Jaramillo, A., Dasi-Espuig, M., Balmaceda, L. A., DeLuca, E. E., Apr. 2013b. Solar Cycle Propagation, Memory, and Prediction: Insights from a Century of Magnetic Proxies. *ApJ*767, L25.
- Muñoz-Jaramillo, A., Sheeley, N. R., Zhang, J., DeLuca, E. E., Jul. 2012. Calibrating 100 Years of Polar Faculae Measurements: Implications for the Evolution of the Heliospheric Magnetic Field. *ApJ*753, 146.
- Navone, H. D., Ceccatto, H. A., 1995. Forecasting chaos from small data sets: a comparison of different nonlinear algorithms. *Journal of Physics A: Mathematical and General* 28 (12), 3381.
- Nevanlinna, H., Kataja, E., Dec. 1993. An extension of the geomagnetic activity index series aa for two solar cycles (1844-1868). *Geophys. Res. Lett.*20, 2703–2706.
- Ng, K. K., Feb. 2016. Prediction Methods in Solar Sunspots Cycles. *Scientific Reports* 6, 21028.
- Nielsen, R. H., 1987. Kolmogorov’s mapping neural network existence theorem. In: *Proceedings of the IEEE First International Conference on Neural Networks* (San Diego, CA). Vol. III. Piscataway, NJ: IEEE, pp. 11–13.
- Ogurtsov, M. G., Jun. 2005a. Modern Progress in Solar Paleoastronomy and Long-Range Solar-Activity Forecasts. *Astronomy Reports* 49, 495–499.
- Ogurtsov, M. G., Sep. 2005b. On the Possibility of Forecasting the Sun’s Activity Using Radiocarbon Solar Proxy. *Sol. Phys.*231, 167–176.

- Oh, K. J., jae Kim, K., 2002. Analyzing stock market tick data using piecewise nonlinear model. *Expert Systems with Applications* 22 (3), 249 – 255.
- Olligschlaeger, A., Gorr, W., 1997. Spatio-temporal forecasting of crime: application of classical and neural network methods. Working Papers of The Heinz School.
- Ossendrijver, M., 2003a. The solar dynamo. *A&A Rev.*11, 287–367.
- Ossendrijver, M., 2003b. The Solar Dynamo: A Challenge for Theory and Observations (Invited review). In: Pevtsov, A. A., Uitenbroek, H. (Eds.), *Current Theoretical Models and Future High Resolution Solar Observations: Preparing for ATST*. Vol. 286 of *Astronomical Society of the Pacific Conference Series*. p. 97.
- Owens, B., Mar. 2013. Long-term research: Slow science. *Nature*495, 300–303.
- Pan, Y., Billings, S., 2008. Neighborhood detection for the identification of spatiotemporal systems. *IEEE Transactions on Systems, Man, and Cybernetics, Part B (Cybernetics)* 38 (3), 846 – 854.
- Pandya, A. S., Kulkarni, D. R., Parikh, J. C., Apr. 1997. Study of time series prediction under noisy environment. In: Rogers, S. K. (Ed.), *Applications and Science of Artificial Neural Networks III*. Vol. 3077 of *Proc. SPIE*. pp. 116–126.
- Park, D.-C., Woo, D.-M., 2009. Prediction of sunspot series using bilinear recurrent neural network. In: *Information Management and Engineering, 2009. ICIME'09. International Conference on*. IEEE, pp. 94–98.

- Park, Y. R., Murray, T. J., Chen, C., Mar. 1996. Predicting sunspots using a layered perceptron neural network. *IEEE Transactions on Neural Networks* 7, 501–505.
- Parker, E. N., 1979. *Cosmical Magnetic Fields: Their Origin and their Activity* (The International Series of Monographs on Physics). Oxford University Press.
- Parlitz, U., Merkwirth, C., Feb. 2000. Prediction of Spatiotemporal Time Series Based on Reconstructed Local States. *Physical Review Letters* 84, 1890–1893.
- Parodi, M. A., Ceccatto, H. A., Piacentini, R. D., García, P. J., 1999. Actividad solar del ciclo 23. Predicción del máximo y fase decreciente utilizando redes neuronales. *Boletín de la Asociación Argentina de Astronomía La Plata Argentina* 43, 23–24.
- Parsapoor, M., Bilstrup, U., Svensson, B., 2015a. Prediction of solar cycle 24. In: *2015 International Joint Conference on Neural Networks, IJCNN 2015*, Killarney, Ireland, July 12-17, 2015. IEEE, pp. 1–8.
- Parsapoor, M., Brooke, J., Svensson, B., 2015b. A new computational intelligence model for long-term prediction of solar and geomagnetic activity. In: Bonet, B., Koenig, S. (Eds.), *Proceedings of the Twenty-Ninth AAAI Conference on Artificial Intelligence*, January 25-30, 2015, Austin, Texas, USA. AAAI Press, pp. 4192–4193.
- Pesnell, W. D., Oct 2008. Predictions of solar cycle 24. *Solar Physics* 252 (1), 209–220.

- Pesnell, W. D., Nov. 2012. Solar Cycle Predictions (Invited Review). Sol. Phys.281, 507–532.
- Petrie, G. J. D., Petrovay, K., Schatten, K., Dec. 2014. Solar Polar Fields and the 22-Year Activity Cycle: Observations and Models. Space Sci. Rev.186, 325–357.
- Petrosian, A., Prokhorov, D., Homan, R., Dasheiff, R., Wunsch, D., 2000. Recurrent neural network based prediction of epileptic seizures in intra-and extracranial eeg. Neurocomputing 30 (1), 201–218.
- Poluianov, S., Usoskin, I., Jun. 2014. Critical Analysis of a Hypothesis of the Planetary Tidal Influence on Solar Activity. Sol. Phys.289, 2333–2342.
- Qi, C., Li, H.-X., 2009. Nonlinear dimension reduction based neural modeling for distributed parameter processes. Chemical Engineering Science 64 (19), 4164 – 4170.
- Quassim, M. S., Attia, A. F., 2005. Forecasting the global temperature trend according to the predicted solar activity during the next decades. Mem. Soc. Astron. Italiana76, 1030.
- Quassim, M. S., Attia, A.-F., Elminir, H. K., Jul. 2007. Forecasting the Peak Amplitude of the 24th and 25th Sunspot Cycles and Accompanying Geomagnetic Activity. Sol. Phys.243, 253–258.
- Reed, R., Marks II, R. J., 1999. Neural Smithing: Supervised Learning in Feedforward Artificial Neural Networks (MIT Press). A Bradford Book.

- Rumelhart, D. E., Hinton, G. E., Williams, R. J., Oct. 1986. Learning representations by back-propagating errors. *Nature*323, 533–536.
- Rumelhart, D. E., McClelland, J. L., Group, P. R., 1986. *Parallel Distributed Processing: Explorations in the Microstructure of Cognition: Foundations (Volume 1)*. A Bradford Book.
- Saad, E. W., Prokhorov, D. V., Wunsch, D. C., 1998. Comparative study of stock trend prediction using time delay, recurrent and probabilistic neural networks. *IEEE Transactions on neural networks* 9 (6), 1456–1470.
- Santos, A. R. G., Cunha, M. S., Avelino, P. P., Campante, T. L., Aug. 2015. Spot cycle reconstruction: an empirical tool. Application to the sunspot cycle. *A&A*580, A62.
- Sauer, T., Yorke, J. A., Casdagli, M., Nov. 1991. Embedology. *Journal of Statistical Physics* 65, 579–616.
- Sauter, T., Weitzenkamp, B., Schneider, C., 2010. Spatio-temporal prediction of snow cover in the black forest mountain range using remote sensing and a recurrent neural network. *International Journal of Climatology* 30 (15), 2330–2341.
- Schatten, K., Nov. 2005. Fair space weather for solar cycle 24. *Geophys. Res. Lett.*32, L21106.
- Schatten, K. H., Scherrer, P. H., Svalgaard, L., Wilcox, J. M., May 1978. Using dynamo theory to predict the sunspot number during solar cycle 21. *Geophys. Res. Lett.*5, 411–414.

- Schatten, K. H., Sofia, S., Jun. 1987. Forecast of an exceptionally large even-numbered solar cycle. *Geophys. Res. Lett.*14, 632–635.
- Schrijver, C. J., Sep. 2015. Socio-Economic Hazards and Impacts of Space Weather: The Important Range Between Mild and Extreme. *Space Weather* 13, 524–528.
- Schwabe, M., Feb. 1844. Sonnenbeobachtungen im Jahre 1843. Von Herrn Hofrath Schwabe in Dessau. *Astronomische Nachrichten* 21, 233.
- Sheng, Z., Hong-Xing, L., Dun-Tang, G., Si-Dan, D., 2003. Determining the input dimension of a neural network for nonlinear time series prediction. *Chinese Physics* 12 (6), 594.
- Shi, D., Zhang, H., Yang, L., 2003. Time-delay neural network for the prediction of carbonation tower's temperature. *IEEE Transactions on Instrumentation and Measurement* 52 (4), 1125–1128.
- Sirvio, K., Hollmén, J., 2008. Spatio-temporal road condition forecasting with markov chains and artificial neural networks. In: *International Workshop on Hybrid Artificial Intelligence Systems*. Springer, pp. 204–211.
- Sitte, R., Sitte, J., 2000. Analysis of the predictive ability of time delay neural networks applied to the s&p 500 time series. *IEEE Transactions on Systems, Man, and Cybernetics, Part C (Applications and Reviews)* 30 (4), 568–572.
- Small, M., Tse, C. K., Dec. 2002. Minimum description length neural networks for time series prediction. *Phys. Rev. E*66 (6), 066701.

- Smaoui, N., Al-Enezi, S., 2004. Modelling the dynamics of nonlinear partial differential equations using neural networks. *Journal of Computational and Applied Mathematics* 170 (1), 27 – 58.
- Solanki, S. K., Usoskin, I. G., Kromer, B., Schüssler, M., Beer, J., Oct. 2004. Unusual activity of the Sun during recent decades compared to the previous 11,000 years. *Nature* 431, 1084–1087.
- Solanki, S. K., Wenzler, T., Schmitt, D., May 2008. Moments of the latitudinal dependence of the sunspot cycle: a new diagnostic of dynamo models. *A&A* 483, 623–632.
- Stathakis, D., 2009. How many hidden layers and nodes? *International Journal of Remote Sensing* 30 (8), 2133–2147.
- Stepanova, M., Antonova, E., Troshichev, O., 2005. Prediction of dst variations from polar cap indices using time-delay neural network. *Journal of atmospheric and solar-terrestrial physics* 67 (17), 1658–1664.
- Sun, Y., Babovic, V., Chan, E. S., 2010. Multi-step-ahead model error prediction using time-delay neural networks combined with chaos theory. *Journal of Hydrology* 395 (12), 109 – 116.
- Svalgaard, L., Cliver, E. W., Kamide, Y., Jan. 2005. Sunspot cycle 24: Smallest cycle in 100 years? *Geophys. Res. Lett.* 32, L01104.
- Takens, F., 1981. Detecting strange attractors in turbulence. *Lecture Notes in Mathematics*, Berlin Springer Verlag 898, 366.

- Tao Cheng, Jiaqiu Wang, X. L., 2008. Space-time series forecasting by artificial neural networks. *Proc.SPIE* 7285, 7285–7285.
- Thompson, R. J., Dec. 1993. A Technique for Predicting the Amplitude of the Solar Cycle. *Sol. Phys.*148, 383–388.
- Uwamahoro, J., McKinnell, L.-A., Cilliers, P. J., Apr. 2009. Forecasting solar cycle 24 using neural networks. *Journal of Atmospheric and Solar-Terrestrial Physics* 71, 569–574.
- Verdes, P., Parodi, M., Granitto, P., Navone, H., Piacentini, R., Ceccatto, H., 2000. Predictions of the maximum amplitude for solar cycle 23 and its subsequent behavior using nonlinear methods. *Solar Physics* 191 (2), 419–425.
- Verdes, P. F., Granitto, P. M., Ceccatto, H. A., May 2004. Secular Behavior of Solar Magnetic Activity: Nonstationary Time-Series Analysis of the Sunspot Record. *Sol. Phys.*221, 167–177.
- Villarreal, J., Baffes, P., Mar. 1990. Sunspot prediction using neural networks. NASA STI/Recon Technical Report N 90.
- Vitinskij, Y. I., 1977. Forecast of the height of solar cycle 21 using methods based on the latitude distribution of sunspots. *Byulletin Solnechnye Dannye Akademii Nauk SSSR* 1976, 59–63.
- Waibel, A., Hanazawa, T., Hinton, G., Shikano, K., Lang, K. J., 1990. Readings in speech recognition. Morgan Kaufmann Publishers Inc., San Francisco, CA, USA, Ch. Phoneme Recognition Using Time-delay Neural Networks, pp. 393–404.

- Wang, W., Li, X., Wang, C., Zhao, H., 2010. River water level forecast based on spatio-temporal series model and rbf neural network. In: Information Science and Engineering (ICISE), 2010 2nd International Conference on. IEEE, pp. 6891–6894.
- Wang, Y.-M., Sheeley, N. R., Mar. 2009. Understanding the Geomagnetic Precursor of the Solar Cycle. *ApJ*694, L11–L15.
- Wang, Z., Bovik, A. C., Jan. 2009. Mean squared error: Lot it or leave it? A new look at Signal Fidelity Measures. *IEEE Signal Processing Magazine* 26, 98–117.
- Wang, Z., Bovik, A. C., Sheikh, H. R., Simoncelli, E. P., 2004. Image quality assessment: From error visibility to structural similarity. *IEEE TRANSACTIONS ON IMAGE PROCESSING* 13 (4), 600–612.
- Wei, H.-L., Billings, S. A., Zhao, Y., Guo, L., 2010. An adaptive wavelet neural network for spatio-temporal system identification. *Neural Networks* 23 (10), 1286–1299.
- Weigend, A. S., 1991. Connectionist Architectures for Time Series Prediction of Dynamical Systems. Ph.D. thesis, STANFORD UNIVERSITY.
- Weigend, A. S., Huberman, B. A., Rumelhart, D. E., 1992. Predicting Sunspots and Exchange Rates with Connectionist Networks. In: Casdagli, M., Eubank, S. (Eds.), *Nonlinear modeling and forecasting*. Addison-Wesley, pp. 395–432.
- Whitney, H., July 1936. Differentiable manifolds. *Ann. Math. (2)* 37 (3), 645–680, mR:1503303. Zbl:0015.32001. JFM:62.1454.01.

- Wik, M., 2008. Multiresolution Analysis and Prediction of Solar Magnetic Flux. In: 37th COSPAR Scientific Assembly. Vol. 37 of COSPAR Meeting. p. 3467.
- Wilson, D., Martinez, T. R., 2003. The general inefficiency of batch training for gradient descent learning. *Neural Networks* 16 (10), 1429 – 1451.
- Wintoft, P., Cander, L. R., 1999. Short-term prediction of fof2 using time-delay neural network. *Physics and Chemistry of the Earth, Part C: Solar, Terrestrial & Planetary Science* 24 (4), 343–347.
- Wu, J., Chan, C. K., 2012. The prediction of monthly average solar radiation with tdnn and arima. In: *Machine Learning and Applications (ICMLA), 2012 11th International Conference on*. Vol. 2. IEEE, pp. 469–474.
- Xie, J.-X., Cheng, C.-T., Chau, K.-W., Pei, Y.-Z., 2006. A hybrid adaptive time-delay neural network model for multi-step-ahead prediction of sunspot activity. *International Journal of Environment and Pollution* 28 (3-4), 364–381.
- Zachilas, L., Gkana, A., 2015. On the verge of a grand solar minimum: A second maunder minimum? *Solar Physics* 290 (5), 1457–1477.
- Zeng, X., Zhang, Y., 2013. Development of recurrent neural network considering temporal-spatial input dynamics for freeway travel time modeling. *Comp.-Aided Civil and Infrastruct. Engineering* 28 (5), 359–371.
- Zhang, G., 2003. Time series forecasting using a hybrid {ARIMA} and neural network model. *Neurocomputing* 50, 159 – 175.

- Zhang, J.-S., Xiao, X.-C., 2000. Predicting chaotic time series using recurrent neural network. *Chinese Physics Letters* 17 (2), 88.
- Zhang, Y., 2009. *Recurrent Neural Networks: Design, Analysis, Applications to Control and Robotic Systems*. LAP Lambert Academic Publishing.
- Zhou, K., Rp, Butler, C., 1998. A statistical study of the relationship between the solar cycle length and tree-ring index values. *Journal of Atmospheric and Solar-Terrestrial Physics* 60 (18), 1711 – 1718.
- Zhou, S., Feng, Y., Wu, W.-Y., Li, Y., Liu, J., Jan. 2014. Low-dimensional chaos and fractal properties of long-term sunspot activity. *Research in Astronomy and Astrophysics* 14, 104–112.